Biomedicine & Pharmacotherapy 153 (2022) 113410

Contents lists available at ScienceDirect

Biomedicine & Pharmacotherapy

journal homepage: www.elsevier.com/locate/biopha

In vivo and *in vitro per se* effect evaluation of Polycaprolactone and Eudragit® RS100-based nanoparticles

Renata Bem dos Santos [a,1], Ana Claudia Funguetto-Ribeiro [a,b,1], Tamara Ramos Maciel [a,c], Dyenefer Pereira Fonseca [e], Fernanda Reis Favarin [b], Daniele Rubert Nogueira-Librelotto [c], Marcelo Gomes de Gomes [a], Tania Ueda Nakamura [d], Clarice Madalena Bueno Rolim [c], Sandra Elisa Haas [a,b,c,*]

[a] *Programa de Pós-Graduação em Ciências Farmacêuticas, Universidade Federal do Pampa, Uruguaiana, RS, Brasil*
[b] *Programa de Pós-Graduação em Bioquímica, Universidade Federal do Pampa, Uruguaiana, RS, Brasil*
[c] *Programa de Pós-Graduação em Ciências Farmacêuticas, Universidade Federal de Santa Maria, Santa Maria, RS, Brasil*
[d] *Departamento de Ciências Básicas da Saúde, Universidade Estadual de Maringá, Maringá, PR, Brasil*
[e] *Departamento de Farmácia, Universidade Estadual de Maringá, Maringá, PR, Brasil*

ARTICLE INFO

Keywords:
Blank nanocapsules
per se effect
Polysorbate 80
PEG
Chitosan
Eudragit

ABSTRACT

Biodegradable polymeric nanocapsules (NC) present incredible characteristics as drug nanocarriers that optimize drug targeting. However, However, a more detailed isolated effect of polymer-based nanoparticles as drug carriers is required. This work aimed to evaluate the *per se* effect of blank-NC (NC-B) with different surface characteristics both *in vitro* and *in vivo* toxicity. NC1-B (Polysorbate 80 coated poly(ε-caprolactone) NC), NC2-B (polyethylene glycol 6000 coated poly(ε-caprolactone) NC), NC3-B (chitosan-coated poly(ε-caprolactone) NC) and NC4-B (Eudragit® RS100 NC) were prepared by nanoprecipitation method. Formulations were characterized by particle size, zeta potential, and pH. The *in vitro* cytotoxicity tests against tumor cell lines were performed (HepG2 and MCF-7). Antiviral activity was evaluated by MTT in Vero cells infected with HSV-1 (KOS strain). I*n vivo* evaluation was performed in apomorphine-induced stereotypy in Wistar rats and locomotor activity distance, head movements, and rearing behavior were measured. NC1-B, NC2-B, NC3-B, and NC4-B had a diameter under 350 nm. The pH and zeta potential of formulations varied according to their coating. For *in vitro* evaluation of antitumor activity and antiviral activity, one-way ANOVA showed no significant differences in cell viability. *In vivo* tests showed low neurological effects. In conclusion, different surface characteristics of NC-B did not demonstrate toxicity against the evaluated cell lines HepG2 and MCF-7, antiviral effect against HSV-1, and the neurological effects in a stereotyping model were low and may be attributed to the *per se* effect of NC-B.

1. Introduction

Nanotechnology focused on drug delivery has been growing exponentially since the beginning of the 21st century, with a wide variety of nanocarriers such as microparticles and colloidal systems (liposomes and nanoparticles). These nanosystems have been designed for the treatment of the most diverse types of pathologies, including cancer [1,2], malaria [3,4], and schizophrenia [5].

Historically, inorganic metallic nanoparticles were the first to be described, in 1857, and are studied for their antimicrobial activity [6] and as photoprotective agents [7], for example. Liposomes are vesicular systems (multilamellar or unilamellar), first described in 1965 [8], presenting micro or nanometric scale, used for the vectorization of lipophilic and/or hydrophilic substances. Since then, other nanosystems have been developed and reported for the diagnosis, cure, and treatment of various conditions, such as dendrimers [9], nanoemulsions [10], nanospheres [11], and nanocapsules [3,12].

Around the year 2000, the synthesis of polymeric nanocapsules (NC) was reported as nanoparticles with submicrometric vesicular systems and moving through Brownian motion. NC are nanoparticles with a spherical shape, in which the lipid matrix (solid or not) is surrounded by a polymeric wall, and they can be functionalized by a variety of coatings

* Correspondence to: Pharmacology and Pharmacometrics Lab – Universidade Federal do Pampa, BR 472, Km 575, 97500–970 Uruguaiana, RS, Brazil.
E-mail address: sandrahaas@unipampa.edu.br (S.E. Haas).
[1] Both authors contributed equally for this work

https://doi.org/10.1016/j.biopha.2022.113410
Received 31 May 2022; Received in revised form 11 July 2022; Accepted 11 July 2022
Available online 15 July 2022

[13,14]. NC can be prepared using different constituents, such as polymers, surfactants, oils, and these variations result in particles with different physicochemical characteristics [14]. The use of different polymers in the production of nanoparticles has been reported to present better physical and biological stability, when compared to liposomes, for example [15,16].

In general, NC are widely used as drug delivery systems, because these nanocarriers can improve technological aspects, such as solubility and stability [16], and optimize the drug targeting to the biophases, from changes in drug bioavailability [16,17], with results a better pharmacological efficacy. Changing the surface characteristics of NC is a promising alternative for biopharmaceutical improvement, enabling controlled and sustained release, altering the pharmacokinetics, and vectoring of the drug [5,18,19].

Poly (ε-caprolactone) (PCL) (Fig. 1A) is a lipophilic polymer widely used in the synthesis of NC, due to its characteristics of biocompatibility, biodegradability, and non-toxicity [20,21]. Due to its non-polar character, surface modifications are necessary to improve its stability in water, such as the insertion of surfactants (*e.g.* Polysorbate 80 (P80), Fig. 1B) or other polymers [22,23]). Anionic polymers, such as polyethylene glycol (PEG) (Fig. 1C), reduce the interaction with opsonins, increasing the blood circulation time of nanoparticles [5]. When used in polymer-drug conjugates (PCL-PEG-drug), they were able to improve drug release at lower pH, allowing greater drug accumulation at tumor sites, for example [24]. In another study, this association reduced parasitemia and can be considered an efficient drug delivery system for the treatment of malaria [25]. As well as the increase in the NC antipsychotic effect of clozapine, a result reinforced by the increase in the half-life ($t_{1/2}$) in the pharmacokinetic (PK) evaluation [5].

Chitosan (CS) (Fig. 1D), a biopolymer obtained from the alkaline deacetylation of chitin [26] is biodegradable, biocompatible, and of low toxicity [27]. Its cationic characteristics favor mucoadhesion [28], allowing greater interaction with negatively charged membranes [29]. Both PEG and CS act as surface modifiers of PCL-based NC and can improve their aqueous stability.

The Eudragit® RS100 (EUD) (Fig. 1E) is a cationic copolymer of polymethyl methacrylate, approved by the U.S. Food and Drug Administration (FDA), water-insoluble, and non-toxic, commonly used to obtain a prolonged release of drugs [29]. Eudragit®, especially RS100, has been shown to improve the performance of polymeric nanocapsules in a comparative study of mucoadhesive properties between PCL nanocapsules, Eudragit® S100 and Eudragit® RS100, the latter showing

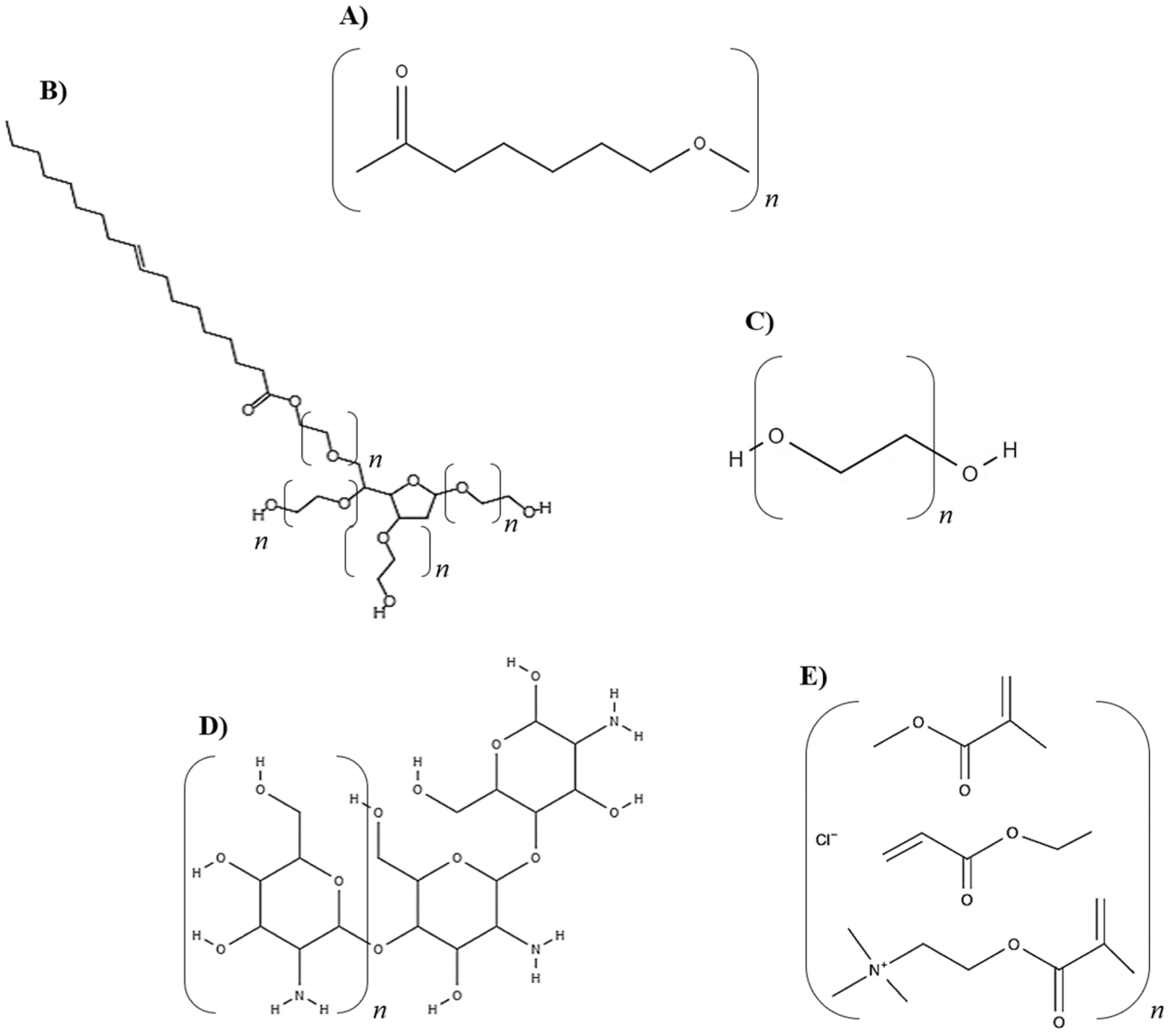

Fig. 1. Chemical structures of (A) Poly (ε-caprolactone) (PCL); (B) Polysorbate 80 (P80); (C) Polyethylene glycol (PEG); (D) Chitosan (CS); and (E) Eudragit® RS 100 (EUD).

superior performance [30]. Eudragit® RS100 nanocapsules improved the *in vitro* antifungal effect of clotrimazole [31], the antioxidant activity of 3,3′-diindolylmethane [32], and the *in vivo* antimalarial activity of quinine [33] showing that cationic charge is important for biological activity.

To develop drugs loaded NC for pharmaceutical purposes, it is advisable to test the activity of these NC without the drugs, to understand if the nanocapsules already have a *per se* activity. NC without drug are also called blank or unload NC (NC-B) and are usually used to evaluate as a negative control of nanoencapsulated drugs [34,35]. However, there are currently few studies that evaluate the activities of NC-B alone and that also evaluate the use of different polymers in their composition [21,36,37].

Our research group developed curcumin-loaded NC with different coatings, using PCL or EUD as polymer [12]. NC-B was used as control. The physical-chemical characterization showed a particle size in the nanometric range, a potential consistent with the coatings used (EUD and CS were cationic; P80 and PEG were anionic). The Differential Scanning Calorimetry (DSC), Fourier-Transform Infrared spectroscopy (FTIR), and X-Ray Powder Diffraction (XRD) analysis reinforced that the coating is on the surface of nanosystem and the predominance of weak interaction forces in the coating and PCL.

Considering that the use of these polymers tends to induce significant changes in the biological performance of nanocarriers; here we characterized and evaluated the *per se* effect of different NC-B in an apomorphine-induced stereotypy model in rats. In addition, it was evaluated, *in vitro*, antitumoral activity against human liver cancer (HepG2) and breast cancer cells (MCF-7); and antiviral activity in African green monkey kidney cells (Vero) infected with Herpes simplex virus type-1 (HSV-1; strain KOS).

2. Materials and methods

2.1. Chemicals

Poly (ε-caprolactone) (PCL, Mw = 80,000 g.mol^{-1}), caprylic/capric triglyceride oil (MCT), sorbitan monostearate (Span® 60), polysorbate 80 (P80), low molecular weight chitosan (CS), Eudragit® RS100 (EUD) and polyethylene glycol 6000 (PEG) were purchased from Sigma-Aldrich (USA). All other chemicals and solvents utilized were of analytical grade. Phosphate buffered saline (PBS), 2,5-diphenyl-3,-(4,5-dimethyl-2-thiazolyl) tetrazolium bromide (MTT), dimethyl sulfoxide (DMSO) and trypsin-EDTA solution (0.5 g porcine trypsin and 0.2 g EDTA • 4Na per liter of Hanks′ Balanced Salt Solution) were obtained from Sigma-Aldrich (USA). Fetal bovine serum (FBS) and Dulbecco's Modified Eagle's Medium (DMEM), supplemented with L-glutamine (584 mg/L) and antibiotic/antimycotic (50 mg/mL gentamicin sulfate and 2 mg/L amphotericin B), were purchased from Vitrocell (Brazil).

2.2. Preparation, characterization, and stability study of NC-B

Blank formulations were prepared with different surface characteristics, using the interfacial deposition of the preformed polymer method [12] (Fig. 2**A**). Each formulation was prepared with a different composition. For NC1-B, an organic phase was composed of PCL (1% w/v), MCT (3.3% v/v) and Span® 60 (0.78% w/v). This phase was dissolved in acetone at 40 ± 1 °C in a water bath, under stirring, and poured into the aqueous phase composed of distilled water and P80 (0.78% w/v), as surfactant. The solvent was evaporated on a rotary evaporator until 10 mL and NC1-B was obtained. For NC2-B formulation, the PEG (0.78%, PEG w/v) was added in the aqueous phase. For NC3-B, a solution of CS (0.5%, w/v) was slowly dripped into the formulation until a final concentration of CS 0.05% (Vieira et al., 2016). For NC4-B formulation, the cationic polymeric nanocapsules were prepared replacing PCL for Eudragit® RS100 and Span® 60 was not added to the formulation [12].

The formulations were characterized about their mean diameter, polydispersity index, zeta potential, pH, and number of particles. The mean diameter and polydispersity were analyzed by laser diffractometry (Mastersizer 2000®, Malvern Instruments, UK). For this analysis, 10 μL of each suspension was diluted in 10 mL of distilled water. For analysis by photon correlation spectroscopy, formulations were diluted in 0.9% NaCl solution (1:100). Zeta potential was determined by electrophoretic migration using Nanobrook 90PlusPals equipment (Brookhaven®). For these determinations, 10 μL of sample was diluted in 10 mL of NaCl solution (1 mmol L^{-1}) and was expressed in millivolts (mV). The pH was analyzed after preparation using a previously calibrated potentiometer (Hanna Instruments, São Paulo, Brazil). The particle number was performed using turbidimetry technique, according to Pereira and collaborators (2019)[37]. The physic-chemical stability was performed on days 0, 10, and 30, evaluating in terms of particle size, zeta potential, and pH. All analyzes were performed in triplicate.

2.3. In vitro evaluation of NC

2.3.1. Cells and virus culture

For the experiments, Vero cells (American Type Culture Collection, ATCC, CCL-81) cultured in DMEM (Dulbecco's Modified Eagle Medium) were used, supplemented with 10% fetal bovine serum (FBS), 100 U/mL penicillin, and 100 U/mL streptomycin. Cell cultures were kept in a

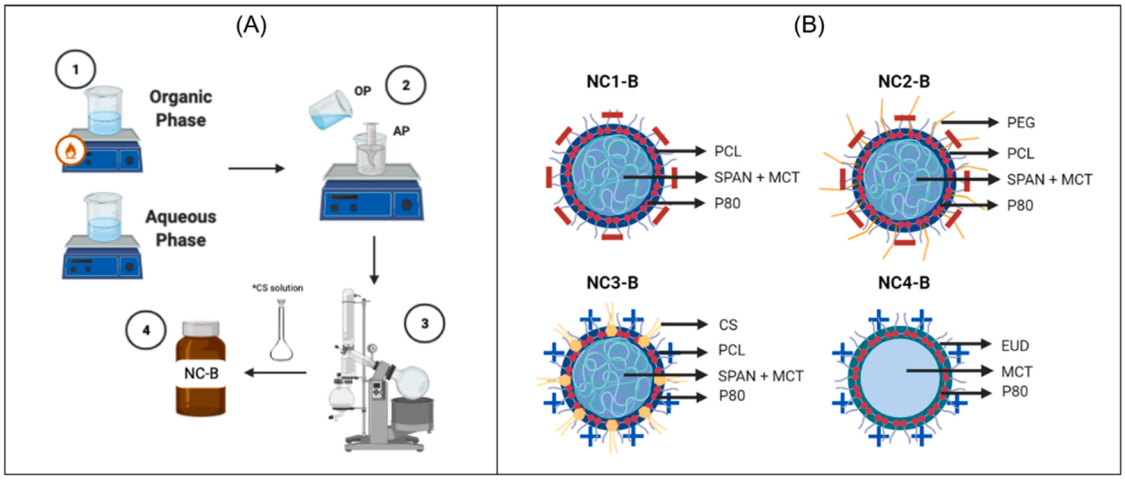

Fig. 2. (A) General scheme of nanoformulation preparation by interfacial deposition of the preformed polymer method; (B) Illustration of structure nanoparticles following the coatings (NC1-B, polysorbate 80; NC2-B, polyethylene glycol; NC3-B, chitosan; NC4-B, Eudragit® RS100).

humid oven at 37 ºC with a tension of 5% CO_2, in plastic cell culture bottles. Cell ringing was performed as recommended by the ATCC (American Type Culture Collection).

The tumor cell lines HepG2, and MCF-7 were grown in DMEM medium (4.5 g/L glucose), supplemented by 10% (v/v) FBS, at 37ºC with 5% CO_2. They were routinely cultured in 75 cm^2 culture flasks and harvested using trypsin-EDTA when the cells reached approximately 80% confluence.

Antiviral activity was evaluated on KOS strain of HSV-1 (clinical isolate of oral lesion sensitive to acyclovir). Viral titers were determined by titration and calculated as 50% tissue culture infectious dose ($TCID_{50}$)/mL, according to the protocol belonging to the Laboratory of Microbiology Applied to Natural and Synthetic Products of Universidade Estadual de Maringá (UEM-Brazil) [38].

2.3.2. Cytotoxicity assay

In cell monolayers, previously formed in 96-well plates, serial dilutions of the samples were added. In sequence, the plate was incubated for 72 h at 37 °C with 5% CO_2. At the end of the incubation period, cell viability was revealed by colorimetric MTT assay as previously described. The absorbance was determined at 570 nm in a microplate reader (Bio-Tek model Power Wave XS). The concentration of 50% cellular cytotoxicity (CC_{50}) of the drugs was calculated by regression analysis of the concentration-response curves.

2.3.3. Antitumor activity

HepG2 (6.5 $\times 10^4$ cells/mL) and MCF-7 (8.5 $\times 10^4$ cells/mL) cell lines were seeded into the 60 central wells of 96-well cell culture plates in 100 µL of complete culture medium. Cells were incubated for 24 h under 5% CO_2 at 37 ºC and the medium was then replaced with 100 µL of fresh medium, supplemented by 5% (v/v) FBS, containing the treatment (NC1-B, NC2-B, NC3-B, or NC4-B) in aliquots of different volumes. Untreated control cells were exposed to a medium with 5% (v/v) FBS only. The cell lines were exposed for 48 h to each treatment, and their viability was assessed by the MTT assay.

The cytotoxicity of each sample in each cell line was expressed as a percentage of viability regarding untreated control cells (the mean optical density of untreated cells was set at 100% viability) and in terms of its IC_{50} (concentration causing 50% death of the cell population).

2.3.4. Antiviral activity

Cell monolayers were prepared in 96-well plates, and, after confluence, the cells were washed with PBS and infected with the $TCID_{50}$ concentration of the viral suspension and incubated for 1 h, 37 °C, 5% CO_2 for viral adsorption. Afterward, two-fold serial dilutions of the infected cells were added. Regarding virus control, only DMEM was added. Incubated again for 72 h, under the conditions already mentioned. At the end of the incubation period, the plates were developed using the MTT colorimetric method. Acyclovir was used as a positive control. The EC_{50} (effective concentration of 50% to inhibit virus-induced cytopathic effect) was determined by regression analysis of the volume of treatment-response curves [38].

2.4. In vivo evaluation of NC

2.4.1. Animals

The experimental protocols for the *in vivo* efficacy were approved by the Animals Ethics Committee of the Federal University of Pampa - UNIPAMPA (036/2018). All the experiments follow the guidelines of the Council for Control of Animal Experiments (CONCEA). Male Wistar rats (90 days old), 200–250 g were purchased from Central Animal Facility of Federal University of Santa Maria. Animals were housed (4 rats/cage) with free access to food (Puro Trato®) and water ad libitum. They were maintained at 22–25 ºC under a 12:12 h light/dark cycle, with lights on at 7:00 a.m.

2.5. Stereotype induced by apomorphine model in rats

2.5.1. Design

To simulate a state of induced psychosis, male Wistar rats (200–250 g, n = 6) received a single dose of apomorphine (APO) as a stereotype-inducer (0.5 mg/kg i.p.) 10 min later of the first treatment. The treatment consisted of saline (control group, NaCl 0.9%) or NC1-B; NC2-B, NC3-B; NC4-B (3.33 mL/kg i.v.) and occurred at two moments: 0 and 40 min

The animals were evaluated individually in an Open Field apparatus (Insight Ltd., Ribeirao Preto, SP, Brazil), for 5 min, at predetermined times. The observations were made by trained researchers at 30 (Time 1 or T1), 60 (Time 2 or T2), 90 (Time 3 or T3), 120 (Time 4 or T4), 150 (Time 5 or T5), and 180 (Time 6 or T6) minutes after the first treatment, as locomotor activity (total distance traveled, number of quadrants) and head movements (number of head elevations) and rearing behavior. Each animal was observed over 5 min [39,40].

2.5.2. Statistical analysis

Data are expressed as means ± S.E.M. Comparisons between groups were performed by one-way analysis of variance (ANOVA), followed by Newman-Keuls Multiple Comparison Test (GraphPad Prism version 6 - San Diego, CA, U.S.A). A value of $p < 0.05$ was considered significant.

3. Results

After preparation, the NC-B were characterized about their mean diameter, polydispersity index, zeta potential, and pH. An illustration of the structure of these nanoparticles is provided in Fig. 2**B**. The results of the mean diameter and zeta potential are presented in Fig. 3 and Fig. 4, respectively. NC-B showed similar diameter characteristics in the nanometer range. The diameters obtained were 199 ± 2, 201 ± 1, 190 ± 2, and 125 ± 1 nm for NC1-B, NC2-B, NC3-B, and NC4-B, respectively. The polydispersity index was less than 2, indicating uniformity in particle size distribution.

The zeta potential values for NC1-B and NC2-B were − 25.3 ± 0.3 and − 25.2 ± 0.1, respectively. The negative charge was due to the anionic characteristics of its coatings. The NC-B coated with CS and EUD showed zeta potential values of 22.1 ± 0.2 and 21.4 ± 0.6, respectively, conferring a positive charge on NC3-B and NC4-B. The formulations showed slightly acidic pH, 5.1 ± 0.03, 5.9 ± 0.03, 4.3 ± 0.01, and 5.3 ± 0.07 for NC1-B, NC2-B, NC3-B, and NC4-B, respectively. The particle number was 3.9 × 10^{12} cm^{-3} for the NC1-B, 3.8 × 10^{12} cm^{-3} for the NC2-B, 2.8 × 10^{12} cm^{-3} for the NC3-B, and 3.7 × 10^{12} cm^{-3} for the NC4-B.

Abbreviations: D0, day 0; D10, day 10; and D30, day 30.

Data are expressed as means ± S.E.M (One-way ANOVA/"Newman-Keuls Multiple Comparison Test").

The results of the physical-chemical stability study are shown in Fig. 5 (A-C). They were analyzed by comparing the parameters of day 0 with the others (10 and 30 days). Regarding particle size (Fig. 5-A), NC1-B and NC4-B showed a significant difference between days 0 and 30 (199 ± 2 and 206 ± 1 nm for NC1-B, and 125 ± 1 and 122 ± 1 nm for NC4-B, respectively). NC3-B showed an increase in size on day 10 (from 201 ± 1 nm on day 0–204 ± 1 nm on day 10), with no change on day 30. NC4-B was stable during the 30 days analyzed.

Zeta potential analyzes (Fig. 5-B) demonstrated, for the anionic NC (NC1-B and NC2-B), changes at day 30 (from −25.3 ± 0.3 mV on day 0 to −21.4 ± 3.7 mV on day 30) and 10 and 30 (−25.2 ± 0.1on day 0, −27.9 ± 0.1 on day 10 and −26.3 ± 0.3 mV on day 30) respectively. The anionic NC (NC3-B and NC4-B) showed changes on day 10 for NC3-B (22.1 ± 0.2 on day 0–17.9 ± 0.2 mV on day 10) and on day 30 for NC4-B (21.4 ± 0.6 on day 0 and 25.2 ± 1.7 mV on day 30). A pH reduction on day 30 was visualized for NC1-B (from 5.17 ± 0.03 on day 0–5 ± 0.03 on day 30), and a decrease followed by an increase on days 10 and 30 for NC2-B (5.95 ± 0.03 on day 30). day 0, 5.83 ± 0.03 on day

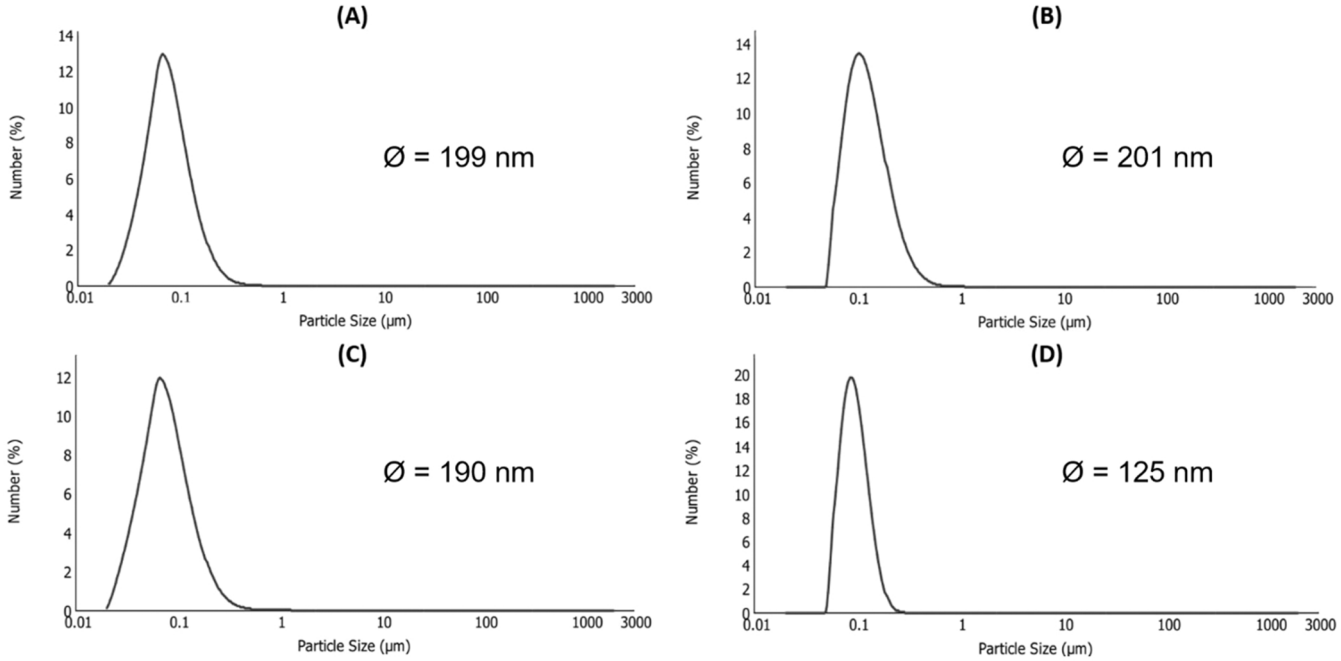

Fig. 3. Diameter of nanocapsules: (A) NC1-B; (B) NC2-B; (C) NC3-B; (D) NC4-B.

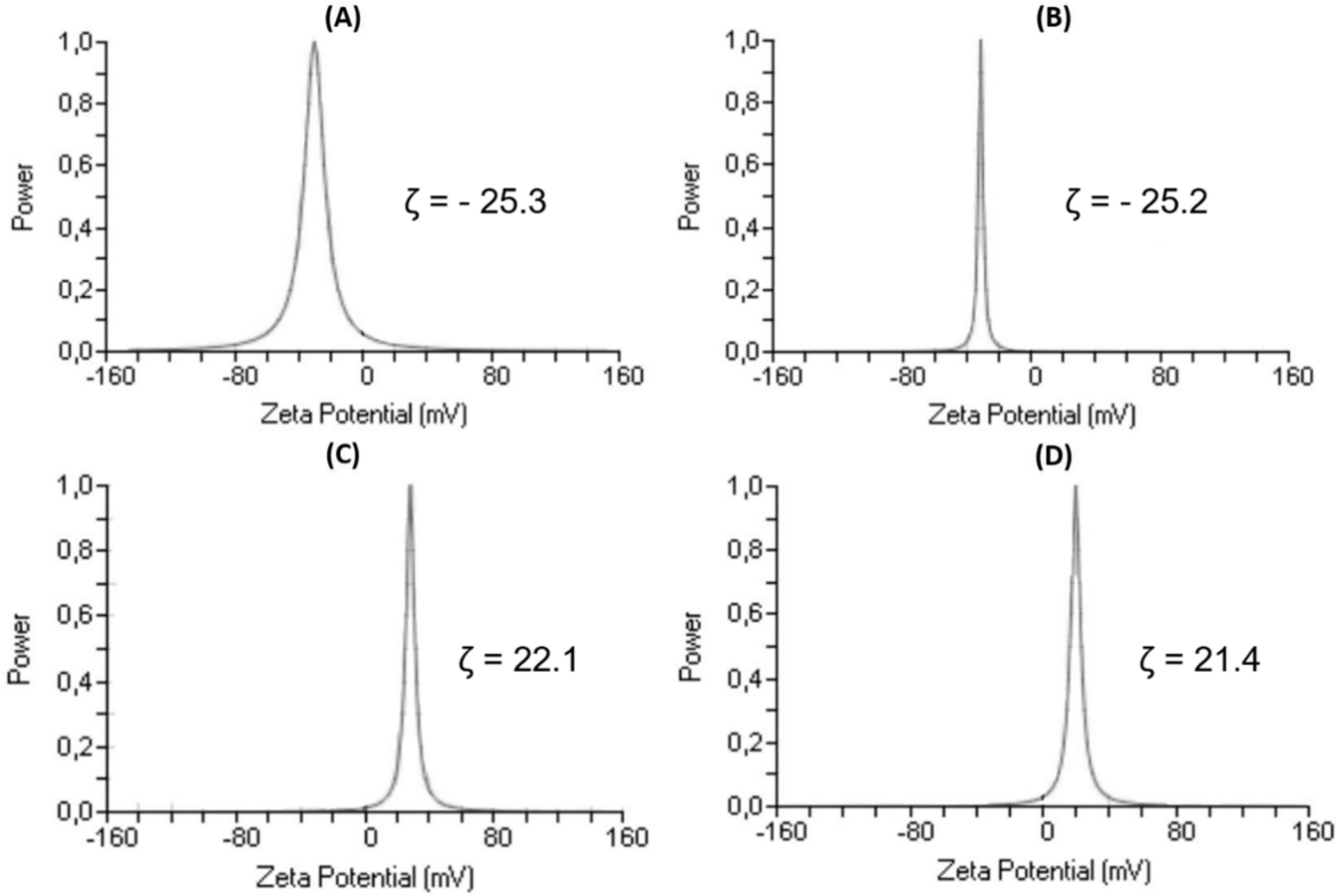

Fig. 4. Zeta potential of nanocapsules: (A) NC1-B; (B) NC2-B; (C) NC3-B; (D) NC4-B.

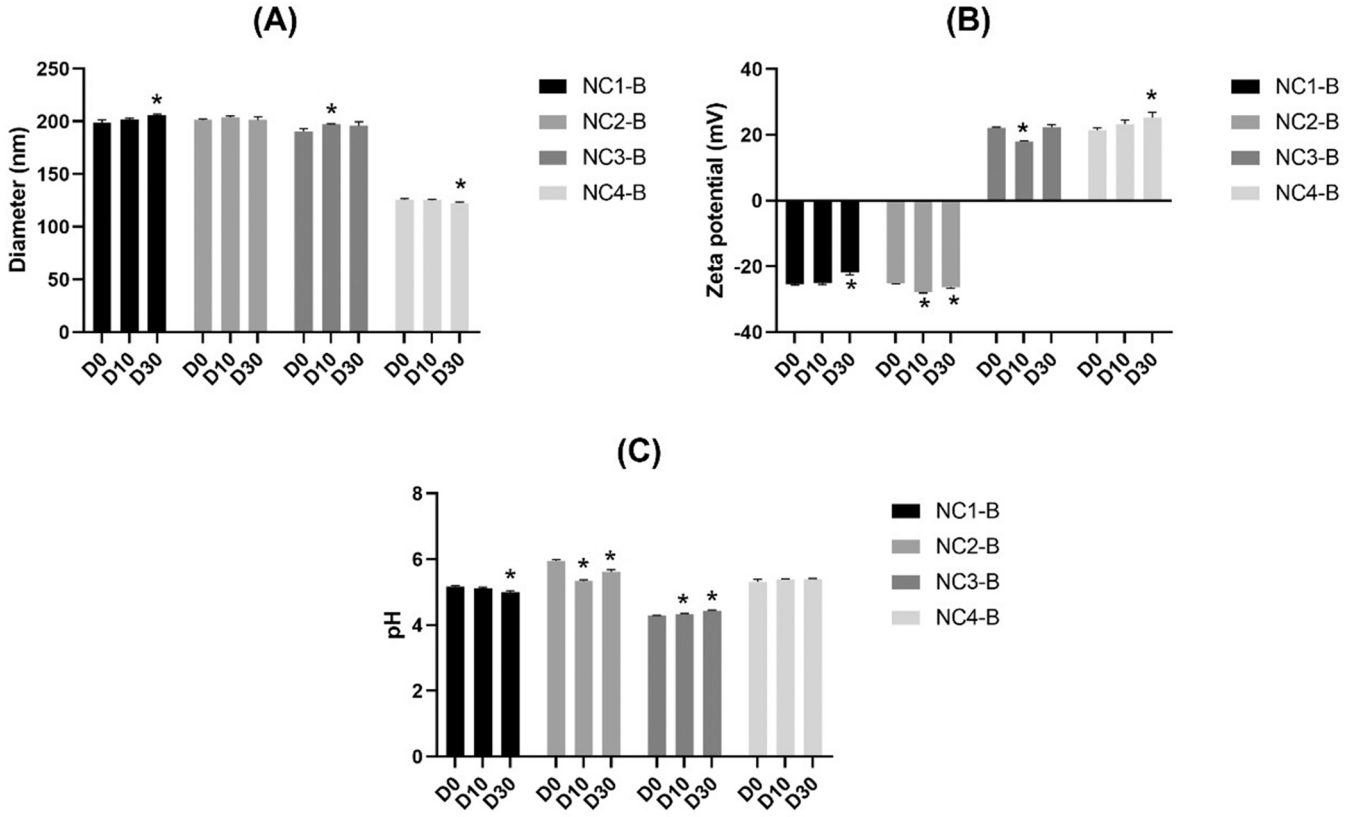

Fig. 5. Physic-chemical stability evaluation of the NC1-B, NC2-B, NC3-B, and NC4-B (A) Particle size; (B) Zeta potential; and (C) pH.

10 and 5.53 ± 0.08 on day 30). NC3-B showed a significant increase on days 10 and 30 (4.29 ± 0.01 on day 0, 4.33 ± 0.02 on day 10, and 4.43 ± 0.02 on day 30), and NC4-B remained unchanged on the analyzed days.

The *in vitro* tests were performed to evaluate the antiviral activity and the antitumor activity of the NC (Table 1**, and** Table 2). For *in vitro* evaluation of antitumor and antiviral activity, one-way ANOVA showed low significant differences in cell viability between the groups. *In vivo* tests of stereotypes induced by apomorphine with NC-B treatment were performed; the distance of locomotor activity, head movements, and the rearing behavior of the animals were evaluated. Fig. 6 shows the results of the stereotype induced by apomorphine test, in terms of total locomotor activity and of all times studied. A one-way ANOVA revealed no significant differences in total locomotor activity and all times studied (Total ($F_{1,36}$ = 1.63, $p < 0.21$, Fig. 6**A**), T1 (30 min) ($F_{1,36}$ = 2.12, $p < 0.12$, Fig. 6**B**), T2 (60 min) ($F_{1,36}$ = 1.44, $p < 0.25$, Fig. 6**C**), T3 (90 min) ($F_{1,36}$ = 1.41, $p < 0.26$, Fig. 6**D**), T4 (120 min) ($F_{1,36}$ = 0.41, $p < 0.74$, Fig. 6**E**), T5 (150 min) ($F_{1,36}$ = 0.73, $p < 0.54$, Fig. 6**F**) and T6 (180 min) ($F_{1,36}$ = 0.48, $p < 0.69$, Fig. 6**G**, respectively). Fig. 7 shows the results of the stereotype induced by apomorphine test, in terms of total head movements and of all times studied.

Similarly, statistical analysis demonstrated no significant differences in total head movements for Time 2, Time 3, Time 4, Time 5 and Time 6 (Total ($F_{1,36}$ = 0.29, $p < 0.83$, Fig. 7**A**), T2 (60 min) ($F_{1,36}$ = 2.72, $p < 0.07$, Fig. 7**C**), T3 (90 min) ($F_{1,36}$ = 1.51, $p < 0.24$, Fig. 7**D**), T4 (120 min) ($F_{1,36}$ = 0.44, $p < 0.72$, Fig. 7**E**), T5 (150 min) ($F_{1,36}$ = 1.78, $p < 0.18$, Fig. 7**F**) and T6 (180 min) ($F_{1,36}$ = 1.34, $p < 0.28$, Fig. 7**G**). For time 1, one-way ANOVA showed a significant difference induced by NC ($F_{1,36}$ = 8.14, $p < 0.001$, Fig. 7**B**). Still, *Post hoc* determinations revealed that NC3-B and NC4-B were effective in blocking of hyperlocomotion APO-induced at time 1, when compared to NC1-B and NC2-B.

For rearing behavior, one-way ANOVA showed a significant difference induced by blank nanoformulations (total rearing, Time 1, Time 2, Time 3, Time 4 and Time 6) (Total ($F_{1,36}$ = 9.31, $p < 0.001$, Fig. 8**A**), T1 (30 min) ($F_{1,36}$ = 11.55, $p < 0.001$, Fig. 8**B**), T2 (60 min) ($F_{1,36}$ = 9.02, $p < 0.001$, Fig. 8**C**), T3 (90 min) ($F_{1,36}$ = 5.09, $p < 0.001$, Fig. 8**D**), T4 (120 min) ($F_{1,36}$ = 8.59, $p < 0.001$, Fig. 8**E**) and T6 (180 min) ($F_{1,36}$ = 8.93, $p < 0.001$, Fig. 8**G**, respectively). Statistical analysis demonstrated no significant differences at time 5 ($F_{1,36}$ = 1.17, $p < 0.34$, Fig. 8**F**). *Post hoc* test showed that NC4-B was not able to block stereotyped head movements APO-caused.

Table 1
In vitro antitumor activity of the nanocapsules.

NC	IC_{50} (*) (HepG2)	IC_{50} (*) (MCF-7)
NC1-B	$3.3 \times 10^{10} \pm 1.1 \times 10^{10}$	$2.6 \times 10^{10} \pm 3.7 \times 10^{9}$
NC2-B	$1.0 \times 10^{11} \pm 8.6 \times 10^{10}$	$4.3 \times 10^{10} \pm 1.5 \times 10^{10}$
NC3-B	$1.7 \times 10^{10} \pm 1.4 \times 10^{10}$	$1.27 \times 10^{10} \pm 1.2 \times 10^{9}$
NC4-B	$5.2 \times 10^{10} \pm 2.7 \times 10^{10}$	$5.5 \times 10^{10} \pm 1.1 \times 10^{10}$

* Number of particles.cm^{-3}; Data are expressed as means ± S.E.M (One-way ANOVA/"Newman-Keuls Multiple Comparison Test").

Table 2
In vitro antiviral activity, cytotoxicity, and selectivity index (SI) of the nanocapsules.

NC	CC_{50} (*) (Vero)	EC_{50} (*) (HSV-1 KOS)	SI
NC1-B	$> 6.5 \times 10^{11}$	–	–
NC2-B	$> 6.3 \times 10^{11}$	–	–
NC3-B	$> 4.7 \times 10^{11}$	–	–
NC4-B	$5.9 \times 10^{11} \pm 1.1 \times 10^{10}$	$2.5 \times 10^{11} \pm 9.2 \times 10^{9}$	2.37

* Number of particles.cm^{-3}; Data are expressed as means ± S.E.M (One-way ANOVA/"Newman-Keuls Multiple Comparison Test").

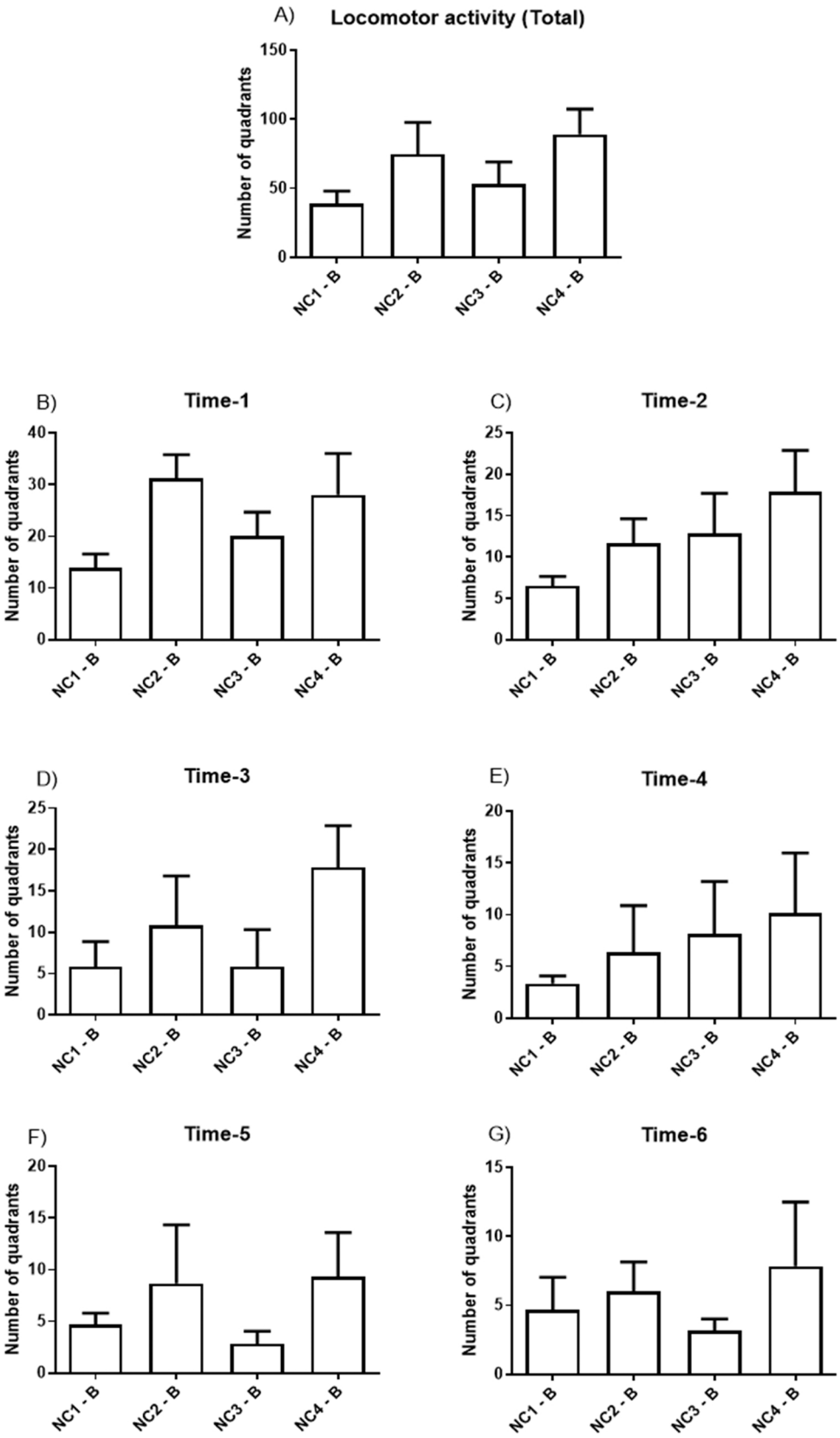

Fig. 6. Evaluation of locomotor activity. **(A)** Total locomotor activity. **(B)** Time 1. **(C)** Time 2. **(D)** Time 3. **(E)** Time 4. **(F)** Time 5. **(G)** Time 6. Data are expressed as means ± S.E.M (One-way ANOVA/"Newman-Keuls Multiple Comparison Test"). * Denoted $p < 0.05$ when compared to NC1-B group. $^{\#}$ Denoted $p < 0.05$ when compared to NC2-B group. $^{@}$ Denoted $p < 0.05$ when compared to NC3-B group.

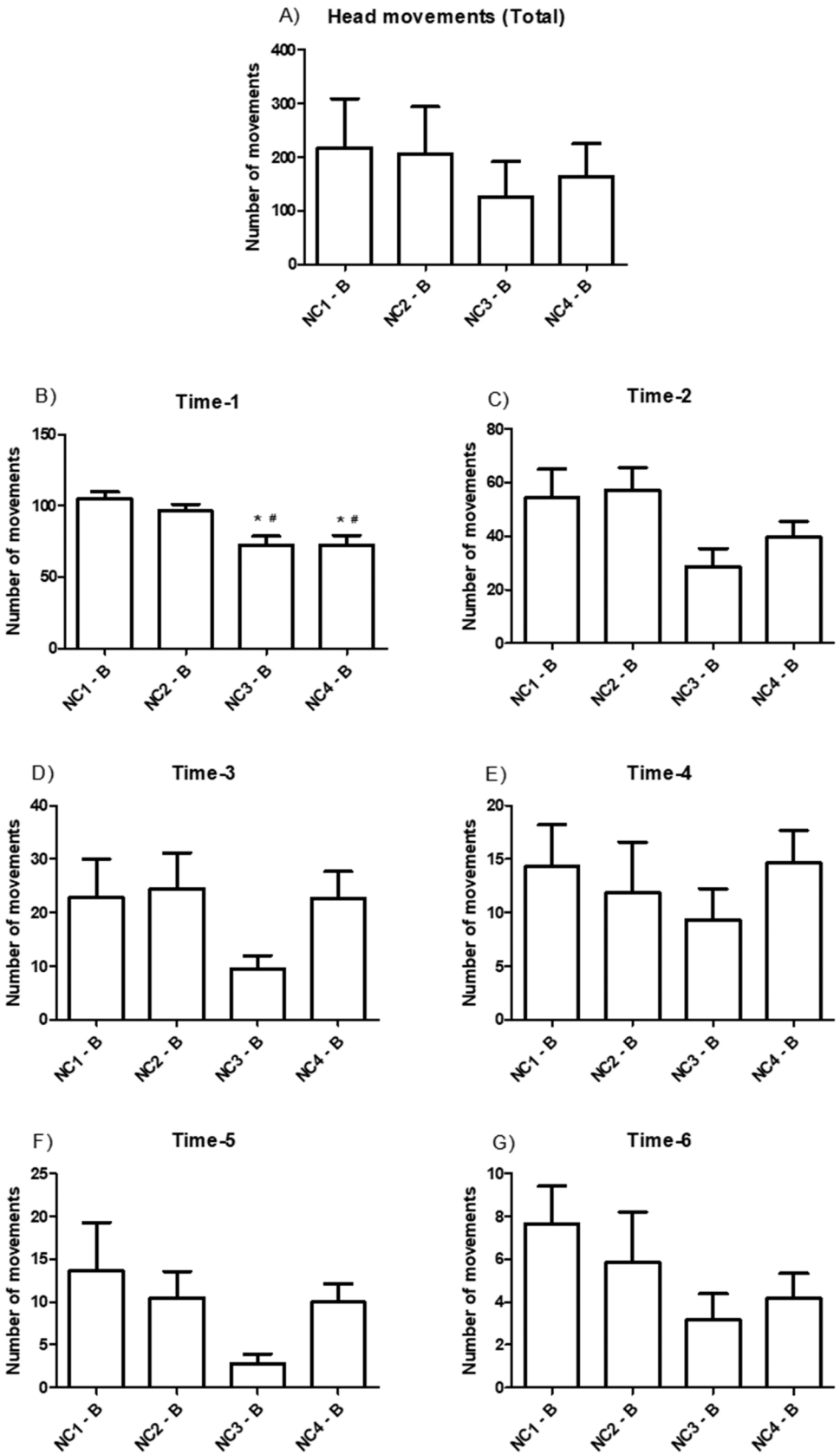

Fig. 7. Evaluation of head movements. **(A)** Total head movements. **(B)** Time 1. **(C)** Time 2. **(D)** Time 3. **(E)** Time 4. **(F)** Time 5. **(G)** Time 6. Data are expressed as means ± S.E.M (One-way ANOVA/"Newman-Keuls Multiple Comparison Test"). * Denoted $p < 0.05$ when compared to NC1-B group. $^{\#}$ Denoted $p < 0.05$ when compared to NC2-B group. $^{@}$ Denoted $p < 0.05$ when compared to NC3-B group.

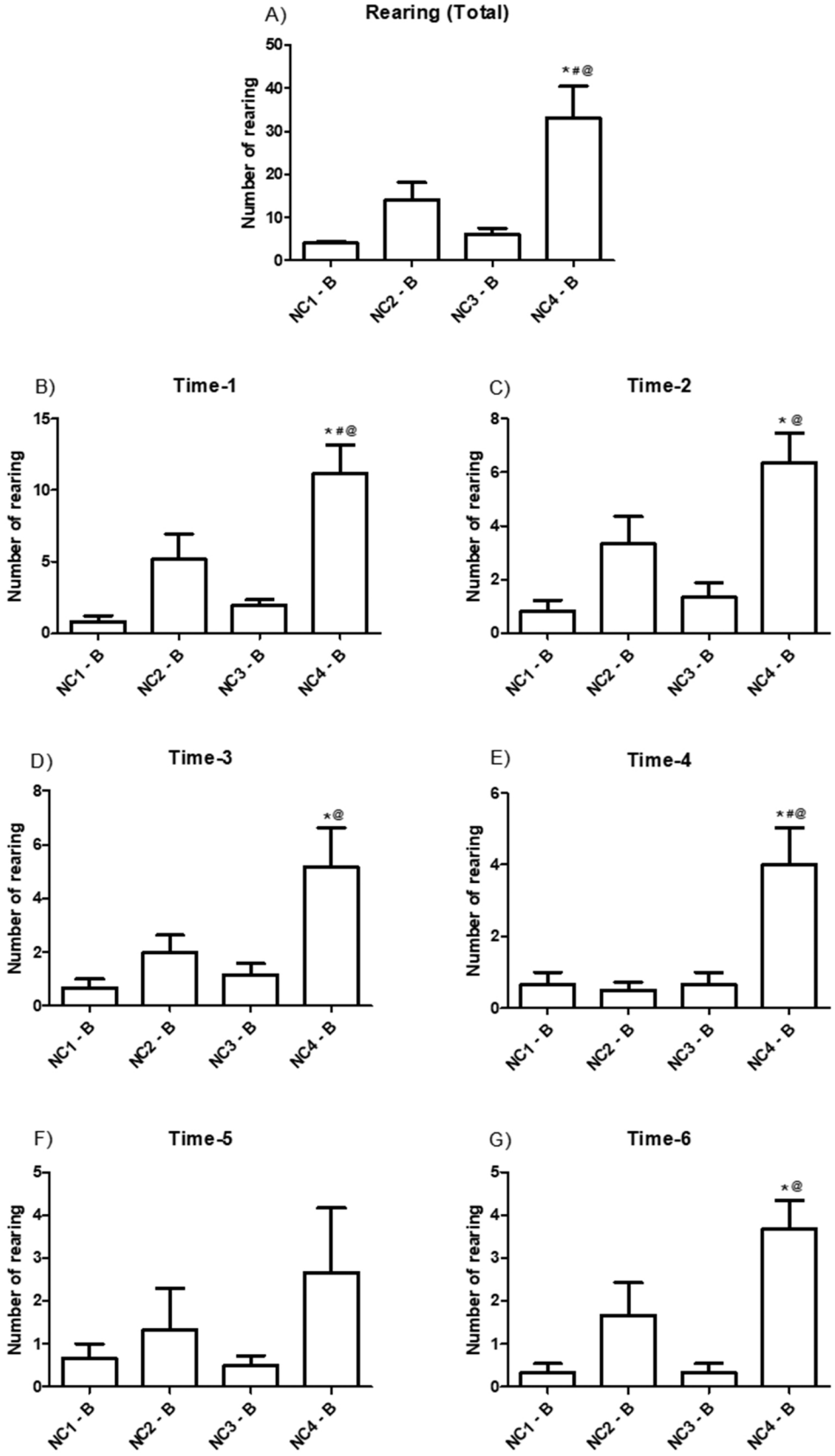

Fig. 8. Evaluation of rearing behavior. **(A)** Total rearing behavior. **(B)** Time 1. **(C)** Time 2. **(D)** Time 3. **(E)** Time 4. **(F)** Time 5. **(G)** Time 6. Data are expressed as means ± S.E.M (One-way ANOVA/"Newman-Keuls Multiple Comparison Test"). * Denoted $p < 0.05$ when compared to NC1-B group. # Denoted $p < 0.05$ when compared to NC2-B group. @ Denoted $p < 0.05$ when compared to NC3-B group.

4. Discussion

In the present study, we investigated the *per se* effect of unloaded NC *in vitro* and *in vivo*. For the *in vitro* study, to evaluate any signs of toxicity and differences between coatings, we used HepG2, MCF-7, Vero cell lines, and HSV-1 KOS strains. The *in vivo* study was carried out in rats previously treated with apomorphine, to induce a pseudo-psychosis state, and treated with different NC-B, to evaluate the difference between coatings in behavioral parameters and the possible *per se* effect.

Several studies address changing the surface characteristics of drugs loaded NC to improve the delivery system, either favoring a controlled release, increasing half-life [5,12], or increasing the effectiveness against pathologies [33]. NC1-B, NC2-B and NC3-B were prepared with PCL as wall. PCL is an aliphatic polyester that is widely used in the manufacture of polymeric nanoparticles due to its well-known characteristics of biocompatibility and slow biodegradation, which allows a controlled and sustained release of drugs, when applicable. All known PCL by-products are totally excreted at the end of the process, which guarantees high safety in the use of this biopolymer [41,42] being FDA approved for the synthesis of biomaterials.

The particle diameters in the present study ranged from 125 to 201 nm, pH from 5.9 to 4.3, and zeta potential from 22.1 to − 25.3 mV. In addition, the number of particles was between 3.9×10^{12} to 2.8×10^{12} cm^{-3}. Although the NC1-B nanoparticles are structurally present with P80 on their surface (Fig. 2**B**), the negative character, evidenced by the zeta potential occurs due to ionization of the PCL carboxylic groups (Fig. 1**A**).

The positive charge of NC3-B (Fig. 2**B**, Fig. 4**C**) is justified by the interaction between the negative charges of PCL, and positive of CS. Similarly, the same is observed with the positive zeta potential of NC4-B, where the surface charge is determined by the cationic character of the polymer EUD (Fig. 2**B**). Izaguirry and collaborators (2016) developed NC-B, with 203 ± 1 nm of size and − 20.1 ± 1.8 mV, also by the interfacial deposition of the preformed polymer method, and the NC-B developed by them is similar to the NC1-B developed in the present work, the only difference among them is the surfactant used, they utilized Lipoid S45® and we utilize Span 60® [36].

NC toxicities can be predicted from physicochemical parameters, such as diameter values, morphology, charge, functional groups, and free energy, and, in this context, the zeta potential is widely used [43]. Generally, cationic particles are more toxic than anionic ones, probably due to the greater cellular interaction with these systems since cells are predominantly anionic [44]. In this study, none of the chemical components showed any effect or toxicity related to the chemical structure (Fig. 1), as well as to the physicochemical parameters evaluated [45–47].

Physico-chemical stability is essential to be evaluated in relation to the storage of formulations [45]. Therefore, the formulations were stored protected from light and at room temperature (± 25 ºC). During the 30 days, the formulations maintained the milky appearance of each formulation, with no changes in color visuals, phase separation, or flocculation.

Particle size must be evaluated due to the tendency of particle aggregate formation and sedimentation over time [46]. To keep these colloidal suspensions stable over time, surfactants such as P80 are used, which have already demonstrated efficiency in maintaining the stability of nanoformulations [47]. Here, despite a small difference in relation to the initial value, all the formulations remained in the nanometric scale and SPAN < 2, not indicating the formation of agglomerates of particles. A similar result was reported by Dos Santos et al. (2015), in which lycopene-loaded NC showed small changes in diameter, but there was no evidence of flocculation in the formulation developed over the evaluated period [48].

Zeta potential is related to the surface charge of the nanoparticles and their stability [48]. NC1-B showed a decrease in values in the module due to P80 auto-oxidation in aqueous medium, forming acetic acid, formic acid, and nonionic acids [49]. In NC2-B, the zeta potential became more negative over time, which may be attributed to water ionization during storage [50]. For NC3-B, zeta potential values changed because of the protonation of the amino groups in the CS structure [51]. Despite the small changes in the zeta potential, values different from zero, once again confirming that there was no agglomeration of the particles over time in all formulations.

The pH measurement is a way of evaluating the chemical stability of the formulation since the degradation of the polymer or another component may be related to the changes in this value [52]. For NC1-B and NC2-B, according to De Sousa Lobato et al. (2013), this reduction can be explained by acidic compounds resulting from P80 self-degradation in aqueous media. Also due to the release of the polyester monomer during the hydrolysis of PCL [53] In contrast, NC3-B showed an increase in pH over time, correlated with zeta potential values, which underwent a reduction in values, being explained by the protonation of the amino groups present[51].

For the *in vitro* analyses, we used mammalian cell and viral isolates. Different cell lines are used in *in vitro* models to evaluate and describe different biological processes in normal and abnormal cells, including therapeutic or toxic agents [54]. Vero is extensively used due to its easy handling, high permissiveness to different xenobiotics, and being a good predictor of cytotoxic agents, besides being genetically and physiologically well-established [54–56].

Cancer cell lines, such as HepG2, and MCF-7 lineage, are popularly used to assess drug toxicity and metabolism, as they have high availability, and proliferation [57]. These cells have been reported to be sensitive to drug nanocarriers, improving the delivery of different molecules, because of enhanced permeation and retention (EPR), that retain the active molecules inside solid tumors [58,59]; however, an isolated investigation of the *per se* effect of polymer-based nanoparticles as drug-carriers is required.

The antiviral activity was analyzed using HSV-1 strains KOS, a lytic virus with high prevalence [60], to investigate the effect of coatings on viral replication. The IC_{50} observed for HepG2 and MCF-7 strains did not show statistically significant differences (1.3×10^{10} to 1.0×10^{11} cm^{-3}). The antiviral effects are evaluated by SI (selectivity index), which showed a value of 2.37 for NC4-B, with a *per se* effect of NC against HSV-1 strains.

In a study carried out by De Gomes and collaborators (2020), the toxicological and behavioral effects of NC-B coated with P80 (NC1-B), CS (NC3-B), EUD (NC4-B), and PEG (NC2-B) in female rats were evaluated. The study was carried out for 14 days, and the animals received the dose daily per oral route (10 mL/kg). Considering that biochemical, histopathological, and behavioral analyzes were performed, it can be demonstrated that there was no significant change in biochemical and histopathological parameters for any of the formulations, and there was also no behavioral change for any of the groups [21]. Another study by Pereira and collaborators (2019), when evaluating the toxicity of the same group of blank nanocapsules (NC1-B, NC2-B, NC3-B, and NC4-B), in male Wistar rats, showed that different general surfaces did not cause alterations in body and organs weight, and histopathological analysis. But when analyzing the lipid profile of the animals, the NC2-B demonstrated an increase in HDL cholesterol levels and NC3-B increased ferric ion reducing antioxidant power levels, with antioxidant action demonstrated in kidneys. As general results, the surfaces demonstrated low or no toxicity in male Wistar rats [37].

De Gomes et al. (2020) and Pereira et al. (2019) investigated the effect of NC-B in an unprecedented way, as they analyzed only these groups, unlike Pacheco et al. (2022) who used NC-B as a negative control for nanocapsules containing curcumin in the experiments. Pacheco et al. (2021) developed anionic and cationic NC coated with d-α-tocopherol 1000 polyethylene glycol succinate (TPGS) and evaluated apomorphine-induced stereotyped behavior in rats. The surface structure used was different from that developed in our work, as it has a copolymer and a co-surfactant in its composition and is functionalized with TPGS. The

dose and route of administration used by them were the same, resulting in changes in total rearing (T3 and T4), head movement (T4), and locomotor activity (T4) of the animals by the NC-B, as well as in our work, in which NC-B also affected rearing behavior (T5) and head movements (T1), whereas NC4-B was not able to block the stereotyped head movements caused by APO. This demonstrates that NC-B may have an effect *per se* and that it may not be an ideal negative control [61].

Izaguirry and collaborators (2016) compared the toxicity of quinine and quinine-loaded nanocapsules (Q-NC) on the reproductive system of male and female rats, and they used NC-B as a negative control in the *in vivo* experiments. The NC-B developed by them is similar to the NC1-B developed in this work, the only difference between them is the surfactant used. And when using the NC-B to evaluate the toxicity in the reproductive system of female and male rats, they found unexpected results, such as alterations in the biochemical parameters of the ovarian and testicular tissues, histological alterations in the testicular tissue, and alterations in the epididymal semen [36]. These results were not expected, as most articles use NC-B as negative controls and do not consider the possibility that these nanoparticles have an effect *per se*.

As already mentioned, nanocarriers improved brain delivery [62]. The stereotype induced by apomorphine model in rats simulates a state of dopaminergic imbalance, common in psychotic conditions, in which hyperexcitation and repetition of movements (stereotyped movements) are observed [63].

The treatments in general did not significantly alter the locomotor activity, head movements, or rearing behavior, in rats with induced stereotypy. But in a specific way, *post hoc* determinations revealed that NC3-B and NC4-B were effective in blocking APO-induced hyperlocomotion at Time 1 (30 min), when compared to NC1-B and NC2-B and that NC4-B was not able to block stereotyped APO-caused head movement.

5. Conclusion

In conclusion, the current study evaluated the effect of NC-B with different polymers (NC1-B, NC2-B, NC3-B, and NC4-B) on *in vitro* cytotoxicity against tumor cell lines, *in vitro* antiviral activity and *in vivo* stereotype test induced by apomorphine in rats. Studies that only assess their effects are of great importance because some polymers used in nanotechnology can improve drug release, pharmacokinetics, and drug targeting profiles. In an unprecedented way, through this study, it was possible to demonstrate that the NC regardless of the coating used, did not demonstrate toxicity against the evaluated cell lines HepG2 and MCF-7, however the treatment with NC4-B proved to be selective against KOS HSV-1 strains. The neurological effects in a stereotyping model in general are low, but they can occur in an isolate way, according to the administered NC-B or evaluated parameter. These effects that occur in isolation may be because effect *per se* and need to be studied in more detail. Thus, further studies are needed to verify the possible mechanisms by which NC coatings can cause behavioral changes *in vivo*.

Funding source

The work was supported by the Rio Grande do Sul Science Foundation (FAPERGS) Grant #19/2551–0001970-0, Coordination for the Improvement of Higher Education Personal, Brazil (CAPES) (#88881.506652/2020-01) and Federal University of Pampa. S.E. Haas is a recipient of the Brazilian National Council for Scientific and Technological Development (CNPq) fellowship (309401/2020-8).

CRediT authorship contribution statement

RB Dos Santos: Conceptualization, Methodology; Investigation; **AC Funguetto-Ribeiro:** Conceptualization, Methodology; Investigation; **TR Maciel:** Investigation; **DP Fonseca:** Investigation, Data curation; **FR Favarin:** Formal analysis, Writing, Data curation; DRN Librelotto: Conceptualization, Supervision; **MG De Gomes:** Formal analysis, Writing. **T Ueda-Nakamura:** Supervision, Funding acquisition; **CMB Rolim:** Supervision, Funding acquisition; **SE Haas:** Conceptualization, Supervision, Funding acquisition.

Conflict of interest

The authors declare that they have no conflict of interest.

References

[1] D. Wang, C. Tu, Y. Su, C. Zhang, U. Greiser, X. Zhu, D. Yan, W. Wang, Supramolecularly engineered phospholipids constructed by nucleobase molecular recognition: upgraded generation of phospholipids for drug delivery, Chem. Sci. 6 (2015) 3775–3787, https://doi.org/10.1039/c5sc01188d.

[2] W. Niu, J. Wang, Q. Wang, J. Shen, D. Wang, C. Tu, Y. Su, C. Zhang, U. Greiser, X. Zhu, D. Yan, W. Wang, Celastrol loaded nanoparticles with ROS-response and ROS-inducer for the treatment of ovarian cancer, Chem. Sci. 8 (2015) 1–9, https://doi.org/10.3389/fchem.2020.574614.

[3] G.S. Gomes, T.R. Maciel, E.M. Piegas, L.R. Michels, L.M. Colomé, R.J. Freddo, D. S. de Ávila, A. Gundel, S.E. Haas, Optimization of curcuma oil/quinine-loaded nanocapsules for malaria treatment, AAPS PharmSciTech 19 (2018) 551–564, https://doi.org/10.1208/s12249-017-0854-6.

[4] K. Velasques, T.R. Maciel, A.H. de Castro Dal Forno, F.E.G. Teixeira, A.L. da Fonseca, F. de, P. Varotti, A.R. Fajardo, D.S. de Ávila, S.E. Haas, Co-nanoencapsulation of antimalarial drugs increases their in vitro efficacy against Plasmodium falciparum and decreases their toxicity to Caenorhabditis elegans, Eur. J. Pharm. Sci. 118 (2018) 1–12, https://doi.org/10.1016/j.ejps.2018.03.014.

[5] S.M. Vieira, L.R. Michels, K. Roversi, V.G. Metz, B.K.S. Moraes, E.M. Piegas, R. J. Freddo, A. Gundel, T.D. Costa, M.E. Burger, L.M. Colomé, S.E. Haas, A surface modification of clozapine-loaded nanocapsules improves their efficacy: a study of formulation development and biological assessment, Colloids Surf. B: Biointerfaces 145 (2016) 748–756, https://doi.org/10.1016/j.colsurfb.2016.05.065.

[6] S. Hamed, M. Emara, R.M. Shawky, R.A. El-domany, T. Youssef, Silver nanoparticles: antimicrobial activity, cytotoxicity, and synergism with N-acetyl cysteine, J. Basic Microbiol. 57 (2017) 659–668, https://doi.org/10.1002/jobm.201700087.

[7] T.G. Smijs, S. Pavel, Titanium dioxide and zinc oxide nanoparticles in sunscreens: focus on their safety and effectiveness, Nanotechnol., Sci. Appl. 4 (2011) 95–112, https://doi.org/10.2147/nsa.s19419.

[8] A.D. Bangham, M.M. Standish, J.C. Watkins, Diffusion of univalent ions across the lamellae of swollen phospholipids, J. Mol. Biol. 13 (1965) 238–252, https://doi.org/10.1016/S0022-2836(65)80093-6.

[9] I. Bargathulla, B. Aadhil Ashwaq, S. Sathiyaraj, A. Sultan Nasar, ElangovanVellaichamy, Pegylated bis-indolyl polyurethane dendrimer: empty drug carrier with prominent anticancer activity, Eur. Polym. J. 153 (2021), 110491, https://doi.org/10.1016/j.eurpolymj.2021.110491.

[10] R.C.S. da Silva, I.R. de Souza Arruda, C.B. Malafaia, M.M. de Moraes, T.S. Beck, C. A. Gomes da Camara, N. Henrique da Silva, M. Vanusa da Silva, M.T. dos Santos Correia, C.P. Frizzo, G. Machado, Synthesis, characterization and antibiofilm/antimicrobial activity of nanoemulsions containing Tetragastris catuaba (Burseraceae) essential oil against disease-causing pathogens, J. Drug Deliv. Sci. Technol. 67 (2022), https://doi.org/10.1016/j.jddst.2021.102795.

[11] J. Yao, J. Liu, H. Zhi, H. Tao, X. Xie, Q. Shi, Surface-modified polylactic acid nanospheres with chitosan for antibacterial activity of 1, 2-benzisothiazolin-3-one, Carbohydr. Polym. 272 (2021), 118406, https://doi.org/10.1016/j.carbpol.2021.118406.

[12] R.B. dos Santos, K.A. Nakama, C.O. Pacheco, M.G. de Gomes, J.F. de Souza, A.C. de Souza Pinto, F.A. de Oliveira, A.L. da Fonseca, F. Varotti, A.R. Fajardo, S.E. Haas, Curcumin-loaded nanocapsules: influence of surface characteristics on technological parameters and potential antimalarial activity, Mater. Sci. Eng. C. 118 (2021), 111356, https://doi.org/10.1016/j.msec.2020.111356.

[13] C.E. Mora-Huertas, H. Fessi, A. Elaissari, Polymer-based nanocapsules for drug delivery, Int. J. Pharm. 385 (2010) 113–142, https://doi.org/10.1016/J.IJPHARM.2009.10.018.

[14] S. Deng, M.R. Gigliobianco, R. Censi, P. di Martino, Polymeric nanocapsules as nanotechnological alternative for drug delivery system: Current status, challenges and opportunities, Nanomaterials 10 (2020) https://doi.org/100.3390/nano10050847.

[15] H. Daraee, A. Etemadi, M. Kouhi, S. Alimirzalu, A. Akbarzadeh, Application of liposomes in medicine and drug delivery, Artif. Cells, Nanomed. Biotechnol. 44 (2016) 381–391, https://doi.org/10.3109/21691401.2014.953633.

[16] S. Davies, R.V. Contri, S.S. Guterres, A.R. Pohlmann, I.C.K. Guerreiro, Simultaneous nanoencapsulation of lipoic acid and resveratrol with improved antioxidant properties for the skin, Colloids Surf. B: Biointerfaces 192 (2020), 111023, https://doi.org/10.1016/j.colsurfb.2020.111023.

[17] F. Carreño, K. Paese, C.M. Silva, S.S. Guterres, T. Dalla Costa, Pharmacokinetic investigation of quetiapine transport across blood–brain barrier mediated by lipid core nanocapsules using brain microdialysis in rats, Mol. Pharm. 13 (2016) 1289–1297, https://doi.org/10.1021/acs.molpharmaceut.5b00875.

[18] C. Shi, S. Zhong, Y. Sun, L. Xu, S. He, Y. Dou, S. Zhao, Y. Gao, X. Cui, Sonochemical preparation of folic acid-decorated reductive-responsive ε-poly-L-lysine-based

microcapsules for targeted drug delivery and reductive-triggered release, Mater. Sci. Eng. C. 106 (2020), 110251, https://doi.org/10.1016/j.msec.2019.110251.
[19] M.G. de Gomes, F.E.G. Teixeira, F.B. de Carvalho, C.O. Pacheco, M.R. da Silva Neto, R. Giacomeli, J.B. Ramalho, R.B. dos Santos, W.B. Domingues, V.F. Campos, S.E. Haas, Curcumin-loaded lipid-core nanocapsules attenuates the immune challenge LPS-induced in rats: Neuroinflammatory and behavioral response in sickness behavior, J. Neuroimmunol. 345 (2020), 577270, https://doi.org/10.1016/j.jneuroim.2020.577270.
[20] D. Mondal, M. Griffith, S.S. Venkatraman, Polycaprolactone-based biomaterials for tissue engineering and drug delivery: Current scenario and challenges, Int. J. Polym. Mater. Polym. Biomater. 65 (2016) 255–265, https://doi.org/10.1080/00914037.2015.1103241.
[21] M.G. de Gomes, M. Pando Pereira, F.E. Guerra Teixeira, F. Carvalho, A.S. Pinto Savall, D. Ferreira Bicca, E. Monteiro Fidelis, P.E. Botura, F. Weber Cibin, S. Pinton, S.E. Haas, Assessment of unloaded polymeric nanocapsules with different coatings in female rats: Influence on toxicological and behavioral parameters, Biomed. Pharmacother. 121 (2020), 109575, https://doi.org/10.1016/j.biopha.2019.109575.
[22] Q.T.H. Shubhra, J. Tóth, J. Gyenis, T. Feczkó, Poloxamers for surface modification of hydrophobic drug carriers and their effects on drug delivery, Polym. Rev. 54 (2014) 112–138, https://doi.org/10.1080/15583724.2013.862544.
[23] M.R. Tavares, L.R. de Menezes, J.C. Dutra Filho, L.M. Cabral, M.I.B. Tavares, Surface-coated polycaprolactone nanoparticles with pharmaceutical application: structural and molecular mobility evaluation by TD NMR, Polym. Test. 60 (2017) 39–48, https://doi.org/10.1016/j.polymertesting.2017.01.032.
[24] K. Rostamizadeh, M. Manafi, H. Nosrati, H. Kheiri Manjili, H. Danafar, Methotrexate-conjugated mPEG-PCL copolymers: a novel approach for dual triggered drug delivery, New J. Chem. 42 (2018) 5937–5945, https://doi.org/10.1039/c7nj04864e.
[25] A. Ramazani, M. Keramati, H. Malvandi, H. Danafar, H. Kheiri Manjili, Preparation and in vivo evaluation of anti-plasmodial properties of artemisinin-loaded PCL–PEG–PCL nanoparticles, Pharm. Dev. Technol. 23 (2018) 911–920, https://doi.org/10.1080/10837450.2017.1372781.
[26] L.B. Prado, S.C. Huber, A. Barnabé, F.D.S. Bassora, D.S. Paixão, N. Duran, J. M. Annichino-Bizzacchi, Characterization of PCL and chitosan nanoparticles as carriers of enoxaparin and its antithrombotic effect in animal models of venous thrombosis, J. Nanotechnol. (2017)) (2017), https://doi.org/10.1155/2017/4925495.
[27] N.P. da Silva, E. do Carmo Rapozo Lavinas Pereira, L.M. Duarte, J.C. de Oliveira Freitas, C.G. de Almeida, T.P. da Silva, R.C.N. de Melo, A.C. Morais Apolônio, M.A. L. de Oliveira, H. de Mello Brandão, F. Pittella, R.L. Fabri, G.D. Tavares, P. de Faria Pinto, Improved anti-Cutibacterium acnes activity of tea tree oil-loaded chitosan-poly(ε-caprolactone) core-shell nanocapsules, Colloids Surf. B: Biointerfaces 196 (2020), https://doi.org/10.1016/j.colsurfb.2020.111371.
[28] P. dos Santos Chaves, L.A. Frank, A. Torge, M. Schneider, A.R. Pohlmann, S. S. Guterres, R.C.R. Beck, Spray-dried carvedilol-loaded nanocapsules for sublingual administration: mucoadhesive properties and drug permeability, Powder Technol. 354 (2019) 348–357, https://doi.org/10.1016/j.powtec.2019.06.012.
[29] P.D.S. Chaves, L.A. Frank, A.G. Frank, A.R. Pohlmann, S.S. Guterres, R.C.R. Beck, Mucoadhesive Properties of Eudragit®RS100, Eudragit®S100, and Poly (ε-caprolactone) nanocapsules: influence of the vehicle and the mucosal surface, AAPS PharmSciTech 19 (2018) 1637–1646, https://doi.org/10.1208/s12249-018-0968-5.
[30] P.D.S. Chaves, L.A. Frank, A.G. Frank, A.R. Pohlmann, S.S. Guterres, R.C.R. Beck, Mucoadhesive Properties of Eudragit®RS100, Eudragit®S100, and Poly (ε-caprolactone) nanocapsules: influence of the vehicle and the mucosal surface, AAPS PharmSciTech 19 (2018) 1637–1646, https://doi.org/10.1208/s12249-018-0968-5.
[31] S.S. Santos, A. Lorenzoni, L.M. Ferreira, J. Mattiazzi, A.I.H. Adams, L.B. Denardi, S. H. Alves, S.R. Schaffazick, L. Cruz, Clotrimazole-loaded Eudragit® RS100 nanocapsules: preparation, characterization and in vitro evaluation of antifungal activity against Candida species, Mater. Sci. Eng. C. 33 (2013) 1389–1394, https://doi.org/10.1016/j.msec.2012.12.040.
[32] J. Mattiazzi, M.H.M. Sari, R. Lautenchleger, M. Dal Prá, E. Braganhol, L. Cruz, Incorporation of 3,3′-diindolylmethane into nanocapsules improves its photostability, radical scavenging capacity, and cytotoxicity against glioma cells, AAPS PharmSciTech 20 (2019) 1–11, https://doi.org/10.1208/s12249-018-1240-8.
[33] L.R. Michels, T.R. Maciel, K.A. Nakama, F.E.G. Teixeira, F.B. de Carvalho, A. Gundel, B.V. de Araujo, S.E. Haas, Effects of surface characteristics of polymeric nanocapsules on the pharmacokinetics and efficacy of antimalarial quinine, Int. J. Nanomed. 14 (2019) 10165–10178, https://doi.org/10.2147/IJN.S227914.
[34] P.T. Ramos, N.S. Pedra, M.S.P. Soares, E.F. da Silveira, P.S. Oliveira, F.B. Grecco, L. M.C. da Silva, L.M. Ferreira, D.A. Ribas, M. Gehrcke, A.O.C. Felix, F.M. Stefanello, R.M. Spanevello, L. Cruz, E. Braganhol, Ketoprofen-loaded rose hip oil nanocapsules attenuate chronic inflammatory response in a pre-clinical trial in mice, Mater. Sci. Eng. C. 103 (2019), 109742, https://doi.org/10.1016/j.msec.2019.109742.
[35] A. Veragten, R.V. Contri, A.H. Betti, V. Herzfeldt, L.A. Frank, A.R. Pohlmann, S.M. K. Rates, S.S. Guterres, Chitosan-coated nanocapsules ameliorates the effect of olanzapine in prepulse inhibition of startle response (PPI) in rats following oral administration, React. Funct. Polym. 148 (2020), 104493, https://doi.org/10.1016/J.REACTFUNCTPOLYM.2020.104493.
[36] A.P. Izaguirry, N.F. Pavin, M.B. Soares, C.C. Spiazzi, F.A. Araújo, L.R. Michels, F. G. Leivas, D.D.S. Brum, S.E. Haas, F.W. Santos, Effect of quinine-loaded polysorbate-coated nanocapsules on male and female reproductive systems of rats, Toxicol. Res. 5 (2016) 1561–1572, https://doi.org/10.1039/c6tx00203j.
[37] M.P. Pereira, M.G. de Gomes, J.C. Izoton, K.A. Nakama, R.B. dos Santos, A.S. Pinto Savall, J.B. Ramalho, S.S. Roman, C. Luchese, F.W. Cibin, S. Pinton, S.E. Haas, Cationic and anionic unloaded polymeric nanocapsules: toxicological evaluation in rats shows low toxicity, Biomed. Pharmacother. 116 (2019), https://doi.org/10.1016/j.biopha.2019.109014.
[38] É. Benassi-Zanqueta, C. Fernandes Marques, S.R. Nocchi, B. Prado, D. Filho, C.V. Nakamura, T. Ueda-Nakamura, Parthenolide Influences Herpes simplex virus 1 Replication in vitro Keywords Caspase·Herpes simplex virus 1·Mitogen-activated protein kinase·NF-κB·Parthenolide, (2018). https://doi.org/10.1159/000490055.
[39] L. Prut, C. Belzung, The open field as a paradigm to measure the effects of drugs on anxiety-like behaviors: a review, Eur. J. Pharmacol. 463 (2003) 3–33, https://doi.org/10.1016/S0014-2999(03)01272-X.
[40] D.M. Benvegnú, R.C.S. Barcelos, N. Boufleur, C.S. Pase, P. Reckziegel, F.C. Flores, A.F. Ourique, M.D. Nora, C.D.B. da Silva, R.C.R. Beck, M.E. Bürger, Haloperidol-loaded polysorbate-coated polymeric nanocapsules decrease its adverse motor side effects and oxidative stress markers in rats, Neurochem. Int. 61 (2012) 623–631, https://doi.org/10.1016/J.NEUINT.2012.06.015.
[41] G.G. Pitt, M.M. Gratzl, G.L. Kimmel, J. Surles, A. Sohindler, Aliphatic polyesters II. The degradation of poly (DL-lactide), poly (ε-caprolactone), and their copolymers in vivo, Biomaterials 2 (1981) 215–220, https://doi.org/10.1016/0142-9612(81)90060-0.
[42] M. Bartnikowski, T.R. Dargaville, S. Ivanovski, D.W. Hutmacher, Degradation mechanisms of polycaprolactone in the context of chemistry, geometry and environment, Prog. Polym. Sci. 96 (2019) 1–20, https://doi.org/10.1016/J.PROGPOLYMSCI.2019.05.004.
[43] M.A. Shahbazi, M. Hamidi, E.M. Mäkilä, H. Zhang, P. v Almeida, M. Kaasalainen, J. J. Salonen, J.T. Hirvonen, H.A. Santos, The mechanisms of surface chemistry effects of mesoporous silicon nanoparticles on immunotoxicity and biocompatibility, Biomaterials 34 (2013) 7776–7789, https://doi.org/10.1016/j.biomaterials.2013.06.052.
[44] C. Ronzani, C. van Belle, P. Didier, C. Spiegelhalter, P. Pierrat, L. Lebeau, F. Pons, Lysosome mediates toxicological effects of polyethyleneimine-based cationic carbon dots, J. Nanopart. Res. 21 (2019), https://doi.org/10.1007/s11051-018-4438-5.
[45] S. Calgaroto, L.E. Fauri, L.A. Frank, K. Paese, S.S. Guterres, A.R. Pohlmann, Chemical stability, mass loss and hydrolysis mechanism of sterile and non-sterile lipid-core nanocapsules: the influence of the molar mass of the polymer wall, React. Funct. Polym. 133 (2018) 161–172, https://doi.org/10.1016/j.reactfunctpolym.2018.09.018.
[46] S.M. Vieira, L.R. Michels, K. Roversi, V.G. Metz, B.K.S. Moraes, E.M. Piegas, R. J. Freddo, A. Gundel, T.D. Costa, M.E. Burger, L.M. Colomé, S.E. Haas, A surface modification of clozapine-loaded nanocapsules improves their efficacy: a study of formulation development and biological assessment, Colloids Surf. B: Biointerfaces 145 (2016) 748–756, https://doi.org/10.1016/j.colsurfb.2016.05.065.
[47] C.G. Venturini, E. Jäger, C.P. Oliveira, A. Bernardi, A.M.O. Battastini, S.S. Guterres, A.R. Pohlmann, Formulation of lipid core nanocapsules, Colloids Surf. A: Physicochem. Eng. Asp. 375 (2011) 200–208, https://doi.org/10.1016/j.colsurfa.2010.12.011.
[48] P.P. dos Santos, K. Paese, S.S. Guterres, A.R. Pohlmann, T.H. Costa, A. Jablonski, S. H. Flôres, A. de, O. Rios, Development of lycopene-loaded lipid-core nanocapsules: physicochemical characterization and stability study, J. Nanopart. Res. 17 (2015), https://doi.org/10.1007/s11051-015-2917-5.
[49] C. de Campo, M. Dick, P. Pereira dos Santos, T.M. Haas Costa, K. Paese, S. Stanisçuaski Guterres, A. de Oliveira Rios, S. Hickmann Flôres, Zeaxanthin nanoencapsulation with Opuntia monacantha mucilage as structuring material: characterization and stability evaluation under different temperatures, Colloids Surf. A: Physicochem. Eng. Asp. 558 (2018) 410–421, https://doi.org/10.1016/j.colsurfa.2018.09.009.
[50] M.L.S. Gomes, N. da Silva Nascimento, D.M. Borsato, A.P. Pretes, J.M. Nadal, A. Novatski, R.Z. Gomes, D. Fernandes, P.V. Farago, S.M.W. Zanin, Long-lasting anti-platelet activity of cilostazol from poly(ε-caprolactone)-poly(ethylene glycol) blend nanocapsules, Mater. Sci. Eng.: C. 94 (2019) 694–702, https://doi.org/10.1016/J.MSEC.2018.10.029.
[51] W. Wang, X. Hao, S. Chen, Z. Yang, C. Wang, R. Yan, X. Zhang, H. Liu, Q. Shao, Z. Guo, pH-responsive Capsaicin@chitosan nanocapsules for antibiofouling in marine applications, Polym. (Guildf.) 158 (2018) 223–230, https://doi.org/10.1016/j.polymer.2018.10.067.
[52] R.S.K. Kishore, S. Kiese, S. Fischer, A. Pappenberger, U. Grauschopf, H.C. Mahler, The degradation of polysorbates 20 and 80 and its potential impact on the stability of biotherapeutics, Pharm. Res. 28 (2011) 1194–1210, https://doi.org/10.1007/s11095-011-0385-x.
[53] K.B. de Sousa Lobato, K. Paese, J.C. Forgearini, S.S. Guterres, A. Jablonski, A. de Oliveira Rios, Characterisation and stability evaluation of bixin nanocapsules, Food Chem. 141 (2013) 3906–3912, https://doi.org/10.1016/j.foodchem.2013.04.135.
[54] P. Senthilraja, K. Kathiresan, In vitro cytotoxicity MTT assay in vero, HepG2 and MCF-7 cell lines study of marine yeast, J. Appl. Pharm. Sci. 5 (2015) 80–84, https://doi.org/10.7324/JAPS.2015.50313.
[55] M.L. Nguyen, E. Gennis, K.C. Pena, J.A. Blaho, Comparison of HEp-2 and vero cell responses reveal unique proapoptotic activities of the herpes simplex virus type 1 a0 gene transcript and product, Front. Microbiol. 10 (2019) 1–19, https://doi.org/10.3389/fmicb.2019.00998.
[56] N. Ammerman, M. Beier-Sexton, A. Azad, Vero cell line maintenance, Curr. Protoc. Microbiol. APPENDIX (2009) 1–10, https://doi.org/10.1002/9780471729259.mca04es11.Growth.

[57] M.T. Donato, L. Tolosa, M.J. Gómez-Lechón, Culture and functional characterization of human hepatoma HepG2 cells, Protoc. Vitr. Hepatocyte Res. (2015), https://doi.org/10.1007/978-1-4939-2074-7_5.
[58] Y. Yao, Y. Zhou, L. Liu, Y. Xu, Q. Chen, Y. Wang, S. Wu, Y. Deng, J. Zhang, A. Shao, Nanoparticle-based drug delivery in cancer therapy and its role in overcoming drug resistance, Front. Mol. Biosci. 7 (2020) 1–14, https://doi.org/10.3389/fmolb.2020.00193.
[59] B. Ding, H. Chen, C. Wang, Y. Zhai, G. Zhai, Preparation and in vitro evaluation of apigenin loaded lipid nanocapsules, J. Nanosci. Nanotechnol. 13 (2013) 6546–6552, https://doi.org/10.1166/jnn.2013.7763.
[60] S.J. Macdonald, H.H. Mostafa, L.A. Morrison, D.J. Davido, Genome sequence of herpes simplex virus 1 strain KOS, J. Virol. 86 (2012) 6371–6372, https://doi.org/10.1128/jvi.00646-12.
[61] C. de Oliveira Pacheco, M.G. de Gomes, M.R. da Silva Neto, A.J.M. Parisotto, R. B. dos Santos, T.R. Maciel, A.C.F. Ribeiro, R. Giacomeli, S.E. Haas, Surface-functionalized curcumin-loaded polymeric nanocapsules could block apomorphine-induced behavioral changes in rats, Pharmacol. Rep. 74 (2022) 135–147, https://doi.org/10.1007/s43440-021-00331-2.
[62] F. Carreño, V.E. Helfer, K.J. Staudt, L.B. Olivo, K. Paese, F.S. Meyer, A. P. Herrmann, S.S. Guterres, S.M.K. Rates, I. Trocóniz, T.D. Costa, Semi-mechanistic pharmacokinetic modeling of lipid core nanocapsules: understanding quetiapine plasma and brain disposition in a neurodevelopmental animal model of schizophrenia, J. Pharmacol. Exp. Ther. 375 (2020) 49–58, https://doi.org/10.1124/JPET.120.000109.
[63] S.L. Dickinson, B. Gadie, I.F. Tulloch, α1- and α2-Adrenoreceptor antagonists differentially influence locomotor and stereotyped behaviour induced by d-amphetamine and apomorphine in the rat, Psychopharmacol. (Berl.) 96 (1988) 521–527, https://doi.org/10.1007/BF02180034.